2007 IEEE International Conference on
Robotics and Automation
Roma, Italy, 10-14 April 2007

Design and Control of a Powered Knee and Ankle Prosthesis

Frank Sup, *Member, IEEE,* Amit Bohara, and Michael Goldfarb , *Member, IEEE*

***Abstract*—This paper describes the design and control of a transfemoral prosthesis with pneumatically powered knee and ankle joints. The current version of the prosthesis serves as a laboratory testbed for purposes of controller development and testing, and as such is tethered for both power and control. A subsequent version will be self-contained, with on-board control and hot gas (monopropellant) actuation. This paper presents the design of the prosthesis prototype, which is in essence a two degree-of-freedom powered robot mechanically attached to a user, and describes an impedance-based control approach that coordinates the motion of the prosthesis and user for the control of level walking. The control approach is implemented on the prosthesis prototype, and experimental results are shown that indicate the effectiveness of the active prosthesis and control approach in restoring fully powered level walking to the user. Finally, an accompanying video demonstrates the functioning prosthesis in level walking.**

I. INTRODUCTION

A. Motivation

DESPITE significant technological advances over the past decade, such as the introduction of microcomputer-modulated damping during swing, commercial transfemoral prostheses remain limited to energetically passive devices. That is, the joints of the prostheses can either store or dissipate energy, but cannot provide net power over a gait cycle. The inability to deliver joint power significantly impairs the ability of these prostheses to restore many locomotive functions, including walking upstairs and up slopes, running, and jumping, all of which require significant net positive power at the knee joint, ankle joint, or both as seen in Fig. 1 [1-8]. Additionally, even during level walking, transfemoral amputees exhibit asymmetric gait kinematics, expend up to 60% more metabolic energy relative to healthy subjects [9], and exert as much as three times the affected-side hip power and torque relative to healthy subjects [1], potentially limiting the quality of life, and likely speeding the onset of degenerative musculoskeletal conditions. All of these barriers to active locomotive functionality can be significantly improved with the development of a prosthesis with power generation capabilities comparable to an actual limb.

Significant challenges underlie the development of powered lower limb prosthesis; primarily, on-board power and actuation capabilities comparable to biological systems. State-of-the-art power supply and actuation technology such as battery/DC motor combinations suffer from low energy density of the power source (i.e., heavy batteries for a given amount of energy), low actuator force/torque density, and low actuator power density (i.e., heavy motor/gearhead packages for a given amount of force or torque and power output). Recent advances in power supply and actuation for self-powered robots, such as the liquid-fueled approaches described in [10-13], offer the potential of significantly improved energetic characteristics relative to battery/DC motor combinations and capable of biological scale energetic and power potential, and thus brings the potential of a powered lower limb prosthesis to the near horizon. This paper describes the design of a prototype transfemoral prosthesis that is intended to ultimately be powered by the liquid-fueled approach described in [10-13].

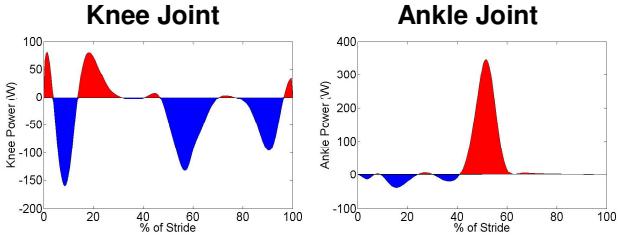

Fig. 1. Joint power during one cycle for a 75 kg normal subject during fast walking. Red represents positive power generated by the joints during level walk [1].

B. Background

Though the authors are not aware of any prior work on the development of a powered knee and ankle prosthesis, prior work does exist on the development of powered knee transfemoral prostheses and powered ankle transtibial prostheses. Regarding the former, Flowers et al. [14-20] developed a tethered electrohydraulic transfemoral prosthesis that consisted of a hydraulically actuated knee joint tethered to a hydraulic power source and off-board electronics and computation. They subsequently developed an "echo control" scheme for gait control, as described by Grimes et al. [16], in which a modified knee trajectory from the sound leg is played back on the contralateral side. In addition to the work directed by Flowers, other groups have also investigated actively powered knee joints for transfemoral prostheses. Specifically, Popovic and Schwirtlich [21] report the development of a

Manuscript received September 15, 2006; revised January 26, 2007. This work was supported in part by the National Science Foundation grant no. CMS0510546. The authors also gratefully acknowledge the support of Otto Bock Healthcare Products for donation of the Lo Rider feet.

The authors are with the Department of Mechanical Engineering, Vanderbilt University, Nashville, TN 37235 USA (e-mail: {frank.c.sup, amit.bohara, michael.goldfarb}@vanderbilt.edu).

battery-powered active knee joint actuated by DC motors, together with a finite state knee controller that utilizes robust position tracking control algorithm for gait control. With regard to active ankle joints, Klute et al. [22, 23] describe the design of an active ankle joint using pneumatic McKibben actuators, although gait control algorithms were not described. Au et al. [24] assessed the feasibility of an EMG based position control approach for a transtibial prosthesis. Finally, though no published literature exists, Ossur, a major prosthetics company based in Iceland, has announced the development of both a powered knee and a self-adjusting ankle. The latter, called the "Proprio Foot," is not a true powered ankle, since it does not contribute power to gait, but rather is used to quasistatically adjust the angle of the ankle to better accommodate sitting and slopes. The powered knee, called the "Power Knee," utilizes an echo control approach similar to the one described by Grimes et al. [16].

Unlike any prior work, this paper describes a prosthesis design that consists of both a powered knee and ankle, and describes a method of control that enables natural, stable, interaction between the user and the powered prosthesis. The control approach is implemented on the prosthesis prototype that is attached to a user, and experimentally shown to provide powered level walking representative of normal gait.

II. Prosthesis Design

To minimize the overall size and weight of the prosthesis, the kinematic configuration of the actuators was selected via a design optimization to minimize the volume of the actuators, subject to the constraints that they provide the requisite range of motion of the joint and provide a torque/angle phase space that accommodates a 75 kg user during fast walking and stair climbing. The data defining the requisite phase space for fast walking and stair climbing were obtained from Winter [1] and Nadeau et al. [3], respectively. Minimum range of motion was determined to be 110° of flexion for the knee and 45° of planterflexion and 20° of dorsiflexion for the ankle. The torque/angle phase space of the resulting knee and ankle actuator configurations are shown graphically in Fig. 2, along with the data for a 75 kg normal human for slow and fast cadences and stair climbing [1, 3].

A. Design Specifications

Figure 3 shows a labeled solid model and photograph, respectively, of the assembled prosthesis prototype. The device incorporates double-acting pneumatic actuators (Bimba model 17-3-DP for the knee joint, model 17-2.75-DP for the ankle). Operating at 2 MPa (300 psig) and controlled by custom four-way servovalves, the actuators are capable of producing 2270 N (510 lbf) of outward axial force, and 2070 N (465 lbf) on the return. It should be noted that heavier users could be accommodated by increasing the operating pressure. The sensor package includes joint torque and position sensors along with a custom 3-axis socket load cell, described in section B, which measures the axial force, sagittal plane moment, and frontal plane moment at the interface between the prosthesis and socket. The torque at each joint is measured via uniaxial load cells (Honeywell Sensotec model 11) located in line with the actuator piston rods. The ankle and knee joints each contain integrated joint motion sensors (ETI Systems model SP12S precision potentiometer). The potentiometers lie inside a pair of Teflon/porous bronze composite dry bearings (Garlock model DU) within each joint.

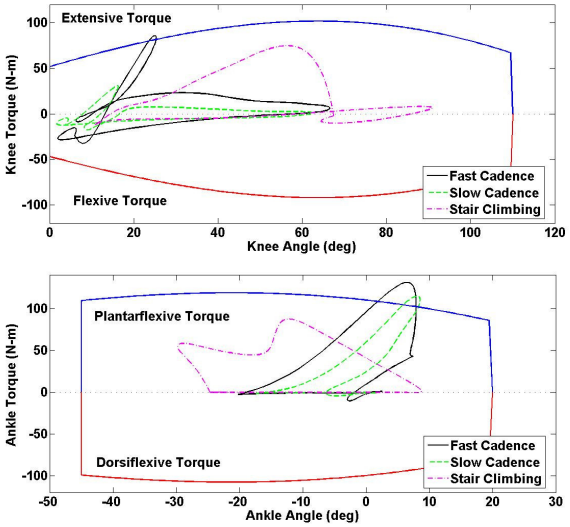

Fig. 2. Comparison of maximum torque capability of active joints to the torque requirement during various gaits for a 75 kg normal user, based on an operating pressure of 2 MPa (300 psig).

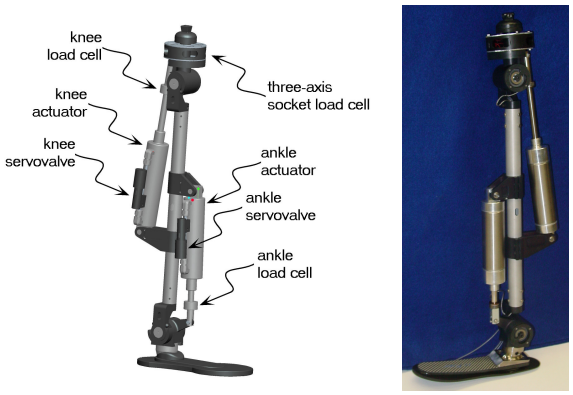

Fig. 3. Major components of power-tethered prototype and actual device.

The structural components of the prosthesis were designed to withstand a 2224 N (500 lbf) load and maximum actuator joint torques using ProE Mechanica finite element analysis (FEA) software to verify safe stress conditions. The results of these analyses indicate that 7075-T6 aluminum, which has a minimum yield strength in excess of 500 MPa, provides a factor of safety between 1.7 and 3.7 for the design conditions.

The active prosthesis was designed to fit a broad range of different sized persons, ranging from two standard deviations below the female norm in length, up to two standard deviations above the male norm in length based on data from Gorden et al. [25]. The tibial length is varied by changing the single structural (tibia) tube and the clamping supports for the

actuators allow for adjustment to achieve the recommended spacing as dictated by the kinematic configuration optimization. The foot is a low profile prosthetic foot (Otto Bock Lo Rider), with typical sizes available. Additionally, the ankle joint and the 3-axis socket load cell incorporate standard pyramid connectors for coupling the prosthesis to the feet and socket, thus enabling a high degree of adjustment in the knee and ankle alignment, as is standard in transfemoral prostheses. Based on actual prosthesis weight and combined with the use of an Otto Bock Lo Rider foot 0.37 kg (0.8 lbf), the total weight of the tethered transfemoral prosthesis with pyramid connectors is 2.65 kg (5.8 lbf), which is within the normal and acceptable range for transfemoral prostheses and less then a comparable normal limb segment [26]. An untethered version is expected to add an additional 0.9 kg (2 lbf). Additional detail, including FEA, of the device design is presented in Sup and Goldfarb [27].

B. Load Cell Design

In addition to joint torque and motion sensors, the prosthesis incorporates a load cell between the prosthesis and user, which measures the interaction forces and moments between the prosthesis and user for purposes of prosthesis control and user intent recognition. Based on the biomechanic data, the range of measurement for the load cell was determined to be 1000 N of axial force (i.e., along the socket) and 100 N-m of sagittal and frontal plane moments. Relative to commercially available multi-axis load cells (e.g., ATI and JR3), this combination of force and moment is disproportionately weighted toward the moment measurement and were physically much larger than could be realistically implemented in a prosthetic leg. As such, a custom load cell was designed and fabricated. The basis of the socket load cell design is a crossed beam, Fig. 4.

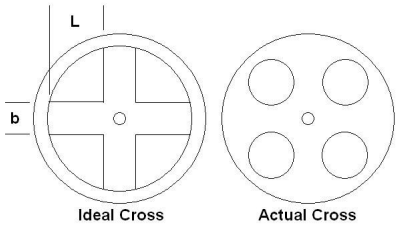

Fig. 4. Ideal versus actual beam patterns of the load cell.

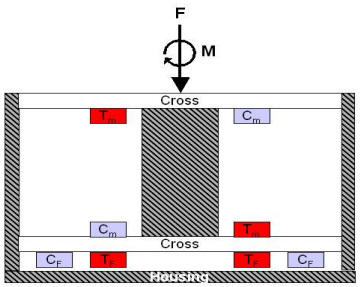

Fig. 5. Regions of compression (C) and tension (T) in a sectional view of the double cross for an applied force, F, and moment, M. Subscripts denote loading responsible for the compression and tension.

The objective of the design is to develop strains of similar magnitudes (e.g., approximately 1000 microstrain for metal foil gages) for a desired applied force and moment. In order to achieve similar magnitudes a double cross configuration, Fig. 5, was developed in order to effectively separate, via a pair of connected crosses, the fundamental mechanisms by which the moment and axial forces are measured. The moment is counteracted by a force couple transmitted by a connecting rod, which loads the beams in tension and compression, while the force is counteracted by loading the beams in bending. The different mechanisms of loading allow the relative geometry of the pair to be manipulated to generate similar strain sensitivity to force and moments. Based on appropriate analytical descriptions of strain, the double load cell was optimized for the smallest overall device size. The resulting strains were then verified via a ProE Mechanica finite element analysis.

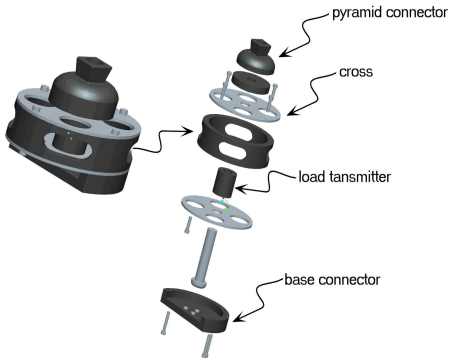

Fig. 6. Assembled and exploded views of the load cell.

The double cross design, which is shown in Fig. 6, consists of two single crosses separated by a distance and rigidly held together by a housing on the outside and load transmitter in the center. The device was fabricated with a final weight of 360 g using the actual cross design as depicted in Fig. 4. Calibration of the device indicated that the loading could not be directly inferred from the raw data due to (mechanical) cross talk between the applied forces and moments. To decouple the cross talk, a least squares method was used to calculate a transformation matrix between the vector of applied forces and moments and measured voltage output from the three bridges based on a fifth-order polynomial. The result of the transformation gave the following results in the axial load a maximum error of 2.2% FSO (1000 N), in the sagittal moment a maximum error of 6.7% FSO (100 Nm) and in the frontal moment a maximum error of 5.5% FSO (100 Nm).

III. GAIT CONTROL STRATEGY

The previously described prosthesis is a fully powered two degree-of-freedom robot, capable of significant joint torque and power, which is rigidly attached to a user. As such, the prosthesis necessitates a reliable control framework for generating required joint torques while ensuring stable and coordinated interaction with the user and the environment.

The overarching approach in all prior work has been to

generate a desired joint position trajectory, which by its nature, utilizes the prosthesis as a position source. Such an approach poses several problems for the control of a powered transfemoral prosthesis. First, the desired position trajectories are typically computed based on measurement of the sound side leg trajectory, which restricts the approach to only unilateral amputees, and also presents the problem of instrumenting the sound side leg and the issue of "odd" number of steps, in which case an echoed step is undesirable. A subtler yet significant issue with position-based control is that suitable motion tracking requires a high output impedance, which forces the amputee to react to the limb rather than interact with it. Specifically, in order for the prosthesis to dictate the joint trajectory, it must assume a high output impedance (i.e., must be stiff), thus precluding any dynamic interaction with the user and the environment.

Unlike prior works, the approach proposed herein utilizes an impedance-based approach to generate joint torques. Such an approach enables the user to interact with the prosthesis by leveraging its dynamics in a manner similar to normal gait [28], and also generates stable and predictable behavior. The essence of the approach is therefore to characterize the knee and ankle behavior with a series of finite states consisting of passive spring and damper behaviors, wherein energy is delivered to the user by switching between appropriate equilibrium positions (of the springs) in each finite state.

A. *Impedance Characterization of Gait*

Based loosely on the notion of impedance control proposed by Hogan [29], the torque required at each joint during a single stride (i.e., period) can be piecewise represented by a series of impedance functions. For example, the stance flexion behavior in knee can be approximated as a linear spring, while the pre-swing knee torque is fairly well described by a non-linear spring. Similarly, during stance, the ankle torque can be approximated using linear and non-linear springs. Such an approach is illustrated in Fig. 7, in which a simple regression fit was performed on the torque-angle data from healthy subjects [1] for the knee and ankle joint during stance, which clearly indicates that the stance phase behavior of each joint can be closely approximated with a piecewise combination of (passive) springs. The addition of piecewise dampers further improves the approximation beyond that shown in Fig. 7. Unlike stance phase, swing phase behavior of knee joint is approximated primarily via damping behavior, as has been the case with many passive transfemoral prostheses. As with more typical impedance control approaches, power can be generated at each joint by controlling the "set point" of each spring. For example, during push-off, the ankle set point can change abruptly from a fairly neutral position to a plantar-flexed position, thus providing power during the push-off phase within the impedance control structure. In addition to enabling interaction between the user and prosthesis, the use of impedance functions to characterize joint behavior renders the prosthesis locally passive. That is, in any given state, the behavior is passive, and will come to rest at a local equilibrium, thus providing a reliable and predictable behavior for the human user.

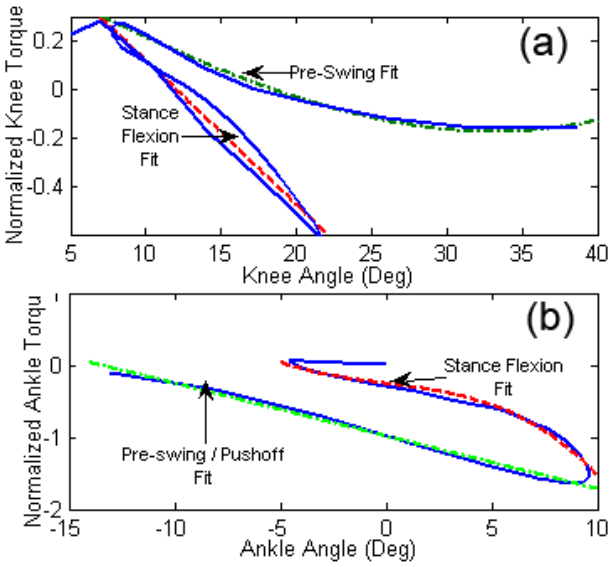

Fig. 7. Stiffness characterization of knee and ankle joint during stance using linear and cubic coefficients. The normalized torques are presented in Nm/kg.

B. *Gait Modes*

The decomposition of joint behavior is performed by dividing normal gait into four main modes or "finite states," as dictated primarily by the piecewise segments of the impedance functions previously described. The stance and swing phase are each divided into two modes as shown in Fig. 8.

Stance 1 begins with heel strike upon which the knee immediately begins to flex so as to provide impact absorption and begin loading, while the ankle simultaneously plantarflexes to reach flat foot. Both knee and ankle joints have relatively high stiffness during this mode to prevent buckling and allow for appropriate stance knee flexion, since stance 1 comprises most of the weight bearing functionality. **Stance 2** is the push-off phase and begins as the ankle dorsiflexes beyond a given angle (i.e., user's center of mass lies forward of stance foot). The knee stiffness decreases in this mode to allow knee flexion while the ankle provides a plantarflexive torque for push off. The push off combined with knee flexion also prepare the leg for the swing phase and hence is also referred to as "Pre-Swing". **Swing 1** begins as the foot leaves the ground as indicated by the load sensors on the prosthetic leg and lasts until the knee reaches maximum flexion. **Swing 2** is active during the extension of the knee joint (i.e., as the lower leg swings forward) which begins as the knee velocity becomes negative and ends at heel strike (as determined by a load sensor). In both the swing modes the ankle power remains passive and is represented in the controller as a (relatively) weak spring regulated to zero degrees. The knee is primarily treated as a damper in both swing 1 and swing 2, while (relatively) weak springs are also

included to aid in swing flexion and prevent high impact velocity at full knee extension in Swing 2, if the dampers alone are found insufficient. A state diagram of the modes is illustrated in Fig. 9.

A general impedance model for each joint within a given mode is represented using a nonlinear spring and damper:

$$\tau = -k_1(\theta - \theta_k) - k_2\theta^3 - b\dot{\theta}. \quad (1)$$

The torque, τ, is written as a function of linear and cubic stiffnesses, k_1 and k_2, and the damping coefficient, b, or a combinations of these. A preliminary set of values for these coefficients obtained from a simple least squares analysis of the population data [1] is shown in Table 1. The parameters shown in Table 1 represents a starting set of values than can be further improved upon via user feedback and joint patterns during gait.

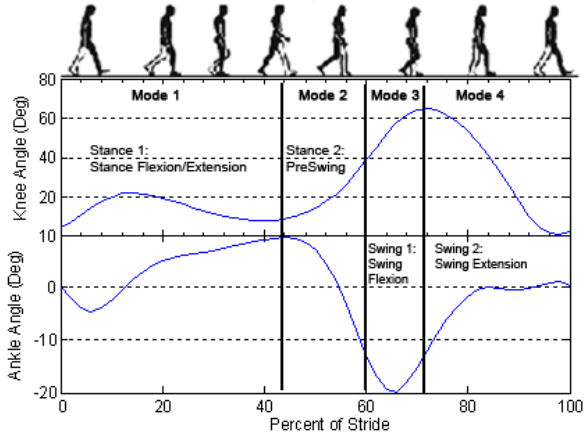

Fig. 8. Subdivision of normal gait into four distinct modes.

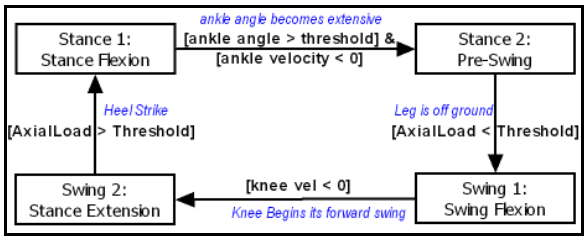

Fig. 9. A finite state model of normal gait. Each box represents a state and the transition condition between states are specified.

TABLE 1: IMPEDANCE PARAMETERS DERIVED FROM A LEAST SQUARES FIT FROM AVAILABLE POPULATION GAIT DATA [1]

MODE	KNEE IMPEDANCE				ANKLE IMPEDANCE			
	k_1	k_2	b	θ_k	k_1	k_2	b	θ_k
Stance 1	4.72	0	0	12	2.96	.07	0	-7
Stance 2	2.48	7e-4	0	16.5	5.6	0	0	-13.5
Swing 1	.05	0	.012	16.8	.1	0	0	0
Swing 2	.54	0	.012	33.5	.1	0	0	0

IV. EXPERIMENTS

The impedance based gait control strategy was implemented on the tethered active prosthesis prototype using an able-bodied testing adaptor as shown in Fig. 10. As shown in the Fig. 10, the adaptor consists of a commercial adjustable locking knee immobilizer (KneeRANGER-Universal Hinged Knee Brace) with an adaptor bracket that transfers load from the subject to the prosthesis. Since the prosthesis remains lateral to the immobilized leg of the healthy subject, the adaptor simulates transfemoral amputee gait without (geometric) interference from the immobilized leg, though minor discomfort was experienced by the user due to an external hip moment resulting from asymmetry in the frontal plane. The prosthesis was tethered to a 2 Mpa (300 psig) pressure source (i.e. compressed nitrogen) and to a controller implemented via a desktop PC.

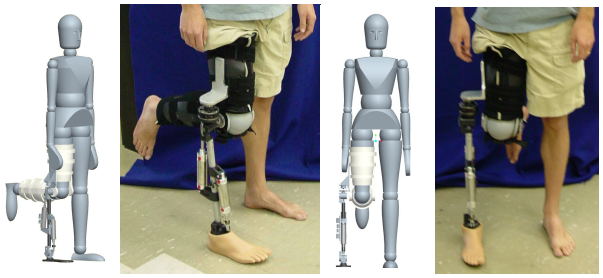

Fig. 10. Able-bodied testing adaptor; enables development, testing, and evaluation of the prosthesis and controllers prior transfemoral amputee participation.

Gait trials were performed on a treadmill, which provided a controlled walking speed of 0.675 m/s (1.5 mph) and enabled enhanced safety monitoring, including the use of handrails and a suspension harness. Tuning of the device was accomplished via joint sensor data, video recordings and most importantly the "feel" of device from the user of the able-bodied adaptor. For example, if the user felt that a joint was not generating necessary torques during support or push off, the stiffness would be increased or the stiffness set point altered. With this recursive process, the impedance functions were tuned. The resulting parameter set is presented in Table 2 and the accompanying video demonstrates the qualitative effectiveness of the device.

TABLE 2: IMPEDANCE PARAMETERS DERIVED EXPERIMENTAL TUNING

MODE	KNEE IMPEDANCE				ANKLE IMPEDANCE			
	k_1	k_2	b	θ_k	k_1	k_2	b	θ_k
Stance 1	3.7	0	0	8	5	.5**	0	-5
Stance 2	2.53	7e-4	0	16	5	0	0	-10
Swing 1	.05	0	.005	16.5	.5	0	0	-1
Swing 2	2.3	0	.012	10*	.75	0	0	-1

*The spring component in swing was turned on when the knee angle approached 10 deg. **The nonlinear component of ankle joint in stance 2 was $0.5*(\theta-2)^3$ and used when $(\theta-2) > 0$.

Measured joint angles and torques from the prosthesis' onboard sensors during level treadmill walking at 0.675 m/s (1.5 mph) are presented in Fig. 11. Note that stance flexion is small due to the relatively slow walking speeds. The knee and ankle joint powers computed directly from the angle and torque data indicate the prosthesis is supplying a significant amount of power to the user. Finally, the measured power from these experiments, shown in Fig. 11, compares favorably to that measured for healthy subjects [1], shown in Fig. 1, thus indicating an enhanced level of functionality relative to

existing passive prostheses. Even greater enhancement of functionality is expected with continued improvement of the control framework.

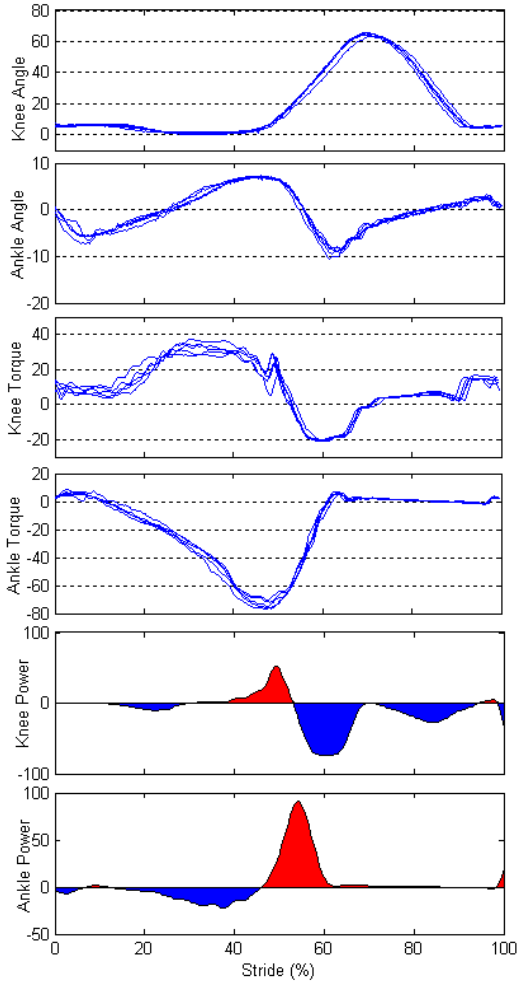

Fig. 11. Measured Joint Angles (Degrees), Joint Torques (N.m), and Averaged Joint Powers (W) for six consecutive gait cycles for a treadmill walk. Average gait cycle period was 1.56s.

REFERENCES

[1] Winter, D.A., "The biomechanics and motor control of human gait: normal, elderly and pathological," University of Waterloo Press, 2nd ed., 1991

[2] Winter, D. A. and Sienko, S. E., "Biomechanics of below-knee amputee gait," *J. of Biomechanics*. 21, 361–367, 1988.

[3] Nadeau, S., McFadyen, B.J., and Malouin, F., "Frontal and sagittal plane analyses of the stair climbing task in healthy adults aged over 40 years: What are the challenges compared to level walking?," *Clinical Biomechanics*, vol. 18, no. 10, pp. 950-959., 2003.

[4] Riener, R., Rabuffetti, M., and Frigo, C., "Joint powers in stair climbing at different slopes," *Proceedings of the IEEE Int. Conf. on Eng. in Medicine and Biology*, vol. 1, p. 530, 1999.

[5] Prilutsky, B.I., Petrova, L.N., and Raitsin, L.M., "Comparison of mechanical energy expenditure of joint moments and muscle forces during human locomotion," *J. of Biomechanics*, vol. 29, no. 4, pp. 405-415, 1996.

[6] DeVita, P., Torry M., Glover, K.L., and Speroni, D.L.,"A Functional Knee Brace Alters Joint Torque and Power Patterns during Walking and Running," *J. of Biomechanics*, vol. 29, no. 5, pp. 583-588, 1996.

[7] Nagano, A., Ishige, Y., and Fukashiro, S., "Comparison of new approaches to estimate mechanical output of individual joints in vertical jumps," *J. of Biomechanics*, vol. 31, no. 10, pp. 951-955, 1998.

[8] Jacobs, R., Bobbert, M.F., van Ingen Schenau, G.J.; "Mechanical output from individual muscles during explosive leg extensions: the role of biarticular muscles," *J. of Biomechanics*, vol. 29, no. 4, pp. 513-523, 1996.

[9] Waters, R., Perry, J., Antonelli, D., and Hislop, H., "Energy cost of walking amputees: the influence of level of amputation," *J. Bone and Joint Surgery*. 58A, 42–46, 1976.

[10] Goldfarb, M., Barth, E.J., Gogola, M.A. and Wehrmeyer, J.A., "Design and Energetic Characterization of a Liquid-Propellant-Powered Actuator for Self-Powered Robots," *IEEE/ASME Trans. on Mechatronics*, vol. 8, no. 2, pp. 254-262, 2003.

[11] Shields, B.L., Fite, K., and Goldfarb, M. Design, Control, and Energetic Characterization of a Solenoid Injected Monopropellant Powered Actuator, *IEEE/ASME Trans. on Mechatronics*, vol. 11, no. 4, pp. 477-487, 2006.

[12] Fite, K.B., Mitchell, J., Barth, E.J., and Goldfarb, M. A Unified Force Controller for a Proportional-Injector Direct-Injection Monopropellant-Powered Actuator, *ASME J. of Dynamic Systems, Measurement and Control*, vol. 128, no. 1, pp. 159-164, 2006.

[13] Fite, K.B., and Goldfarb, M. Design and Energetic Characterization of a Proportional-Injector Monopropellant-Powered Actuator, *IEEE/ASME Trans. on Mechatronics*, vol. 11, no. 2, pp. 196-204, 2006.

[14] Flowers, W.C., "A Man-Interactive Simulator System for Above-Knee Prosthetics Studies," Dept. of Mechanical Engineering PhD Thesis, MIT, 1973.

[15] Donath, M., "Proportional EMG Control for Above-Knee Prosthesis'," Dept. of Mechanical Engineering Masters Thesis, MIT, 1974.

[16] Grimes, D. L., "An Active Multi-Mode Above Knee Prosthesis Controller," Dept. of Mechanical Engineering PhD Thesis, MIT, 1979.

[17] Grimes, D. L., Flowers, W. C., and Donath, M., "Feasibility of an active control scheme for above knee prostheses," *ASME J. of Biomechanical Engineering*, vol. 99, no. 4, pp. 215-221, 1977.

[18] Stein, J.L., "Design Issues in the Stance Phase Control of Above-Knee Prostheses," Dept. of Mechanical Engineering PhD Thesis, MIT, 1983.

[19] Stein, J.L., and Flowers, W.C., "Stance phase control of above-knee prostheses: knee control versus SACH foot design," *J. of Biomechanics*, vol. 20, no. 1, pp. 19-28, 1988.

[20] Flowers, W.C., and Mann, R.W., "Electrohydraulic knee-torque controller for a prosthesis simulator," *ASME J. of Biomechanical Engineering*, vol. 99, no. 4, pp. 3-8., 1977.

[21] Popovic, D. and Schwirtlich, L., "Belgrade active A/K prosthesis, " in de Vries, J. (Ed.), Electrophysiological Kinesiology, Interm. Congress Ser. No. 804, *Excerpta Medica*, Amsterdam, The Netherlands, pp. 337–343, 1988.

[22] Klute, G.K., Czerniecki, J., Hannaford, B., "Development of Powered Prosthetic Lower Limb," Proceedings of the First National Meeting, Veterans Affairs Rehabilitation Research and Development Service, 1998.

[23] Klute, G.K., Czerniecki, J., Hannaford, B., "Muscle-Like Pneumatic Actuators for Below-Knee Prostheses, *Proceedings the Seventh Int. Conf. on New Actuators*, pp. 289-292, 2000.

[24] Au, S. Bonato, P., Herr, H., "An EMG-Position Controlled System for an Active Ankle-Foot Prosthesis: An Initial Experimental Study," *Proceedings of the IEEE Int. Conf. on Rehabilitation Robotics*, pp. 375-379, 2005.

[25] Gordon, CC, B. Bradtmiller, T. Churchill, C.E. Clauser, J.T. McConville, I. Tebbetts and R. Walker, "1988 Anthropometric Survey of US Army Personnel: Methods and Summary Statistics," Technical Report NATICK/TR-89/044, U.S. Army Natick Research, Development and Engineering Center, Natick, MA, 1989.

[26] Clauser CE, McConville JT, Young JM, "Weight, volume and center of mass of segments of the human body." AMRL-TR-69-70, Wright Patterson Airforce Base, Dayton, Ohio, 1969.

[27] Sup, F. and Goldfarb, M., "Design of a Pneumatically Actuated Transfemoral Prosthesis," *Proceedings of the ASME Int. Mech. Eng. Congress and Exposition*, IMECE2006-15707, 2006.

[28] Mochon, S., and McMahon, T.A. Ballistic Walking, *J. of Biomechanics*, vol. 13, no. 1, pp. 49-57, 1980.

[29] Hogan, N., "Impedance Control: An approach to manipulation: Part 1 - theory, Part 2 - Implementation, and Part 3 - Applications," *ASME J. of Dynamic Systems, Measurement and Control*, vol. 107, pp. 1-24, 1985.